

# Synthesis and Aldose Reductase Inhibitory Activities of Novel *N*-Nitromethylsulfonanilide Derivatives

Jun Inoue,<sup>a</sup> Ying-She Cui,<sup>a,\*</sup> Osamu Sakai,<sup>a</sup> Yoshikuni Nakamura,<sup>a</sup>  
Hiromi Kogiso<sup>a</sup> and Peter F. Kador<sup>b</sup>

<sup>a</sup>Research Laboratory, Kobe Creative Center, Senju Pharmaceutical Co., Ltd, 1-5-4 Murotani, Nishi-Ku, Kobe, Hyogo 651-2241, Japan

<sup>b</sup>Laboratory of Ocular Therapeutics, National Eye Institute, National Institutes of Health, Bethesda, MD 20892, USA

Received 26 April 2000; accepted 3 June 2000

**Abstract**—A novel series of 14 *N*-nitromethylsulfonanilide derivatives were synthesized and evaluated for their ability to inhibit recombinant aldose reductase. Computational docking simulations provided a good explanation for the observed structure–activity relationships. Kinetic analysis of (2-fluoro-5-methyl-*N*-methyl)-*N*-nitromethylsulfonanilide, **11**, one of the most potent compounds in this series with an  $IC_{50} = 0.35 \mu M$ , showed uncompetitive inhibition. Subsequent in vitro culture studies of rat lenses with **11** indicated that this series of aldose reductase inhibitors are effective in either preventing or retarding sugar cataract formation associated with diabetes. © 2000 Elsevier Science Ltd. All rights reserved.

## Introduction

Aldose reductase (alditol;  $NADP^+$  oxidoreductase, E.C. 1.1.1.21, ALR2), the first enzyme in the polyol pathway, utilizes NADPH to reduce the aldehyde form of glucose to its respective sugar alcohol, sorbitol. Subsequently, sorbitol dehydrogenase (*L*-iditol;  $NAD^+$  5-oxidoreductase, E.C. 1.1.1.14, SD), the second enzyme in the pathway, utilizes  $NAD^+$  to convert sorbitol to fructose.<sup>1</sup> In diabetes, the increased flux of glucose through the polyol pathway can result in altered cellular redox potentials and increased intracellular levels of sorbitol which results in hyperosmotic stress, cellular swelling and increased membrane permeability and perturbation of membrane transport processes. These changes can initiate cellular lesions associated with late-onset diabetic complications such as neuropathy, nephropathy, keratopathy, angiopathy, and cataract.<sup>1–3</sup> Experimental studies indicate that aldose reductase inhibitors (ARIs), which block the flux of the glucose through polyol pathway and prevent the intracellular accumulation of sorbitol, can prevent, retard, or reverse these complications of chronic diabetes.<sup>1,2</sup> Over the past 30 years, world-wide efforts have been made in the development of clinically useful ARIs. While a number of ARIs have been

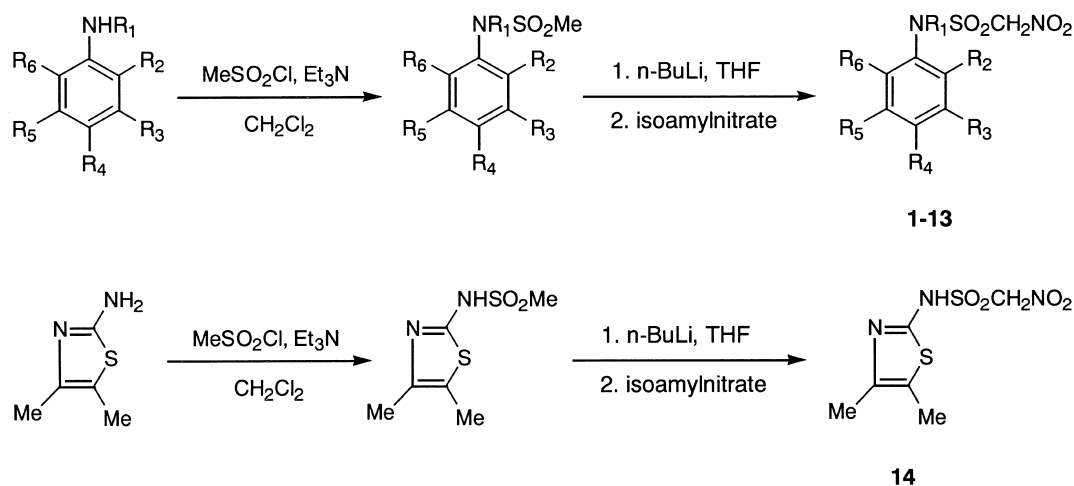
synthesized and identified as potential inhibitors,<sup>2,4–7</sup> many of these compounds have failed clinically due to inadequate efficacy, adverse pharmacokinetics properties, or toxic side-effects. To date, two general series of ARIs have been developed—those possessing a carboxylic acid group and those containing a cyclic imide ring—the latter of which possesses more favorable pharmacokinetics properties.<sup>8,9</sup>

The use of sulfonylnitromethanes as potential ARIs were first reported by Brittain et al.<sup>10</sup> Based on published pharmacophore requirements,<sup>11,12</sup> a new series of *N*-nitromethylsulfonanilide derivatives were designed and synthesized. They were subsequently evaluated for their in vitro ability to inhibit aldose reductase and the observed structure–activity relationships were analyzed using computational docking simulation.

## Results and Discussion

The general route for the synthesis of the *N*-nitromethylsulfonanilide derivatives is illustrated in Scheme 1. The methanesulfonyl group was introduced into the starting arylamine or *N*-alkylaniline by treating methanesulfonyl chloride in the presence of triethylamine. The resulting methanesulfonamide was treated with *n*-butyllithium at  $-10^\circ C$ , followed by reaction with isomyl nitrate at  $-30^\circ C$  to afford the nitromethylsulfonamide.

\*Corresponding author. Tel.: +81-78-997-1010; fax: +81-78-997-1016; e-mail: yingshe-cui@senju.co.jp



Scheme 1.

The newly synthesized compounds were evaluated for their ability to inhibit the *in vitro* reduction of glyceraldehydes by recombinant human muscle aldose reductase which was spectrophotometrically followed by following the consumption of NADPH cofactor at 340 nm. Appropriate controls were employed to negate potential changes in the absorption of nucleotide and/or protein modification reagents or aldose reductase inhibitors at 340 nm in the absence of substrate. The *in vitro* inhibitory activities of these compounds compared to SG210<sup>13</sup> are summarized in Table 1.

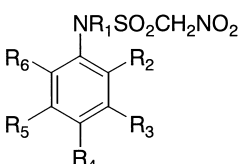
To explain the observed structure–activity relationships, these compounds were docked into the crystal structure of aldose reductase with NADP<sup>+</sup>.glucose-6-phosphate

reported by Harrison et al.<sup>14</sup> and deposited in the Protein Data Bank (code 2ACQ). Minimization of the molecules was conducted by using the Tripos force field with the Powell method,<sup>15</sup> and docking simulations were performed by using the Tripos docking programs FlexX<sup>TM</sup> and FlexiDock<sup>TM</sup>.<sup>16</sup> The enzyme–inhibitor interactions in FlexX include both polar (hydrogen bond and charge–charge) and non-polar (hydrophobic) terms. Many of these interactions are geometrically quite restrictive, which allows FlexX to accurately place inhibitors and their fragments. Directly docking a potential inhibitor into the active site of the enzyme which covers all possible docking combinations of inhibitor conformations and binding modes, and an induced fit could be explored by FlexiDock, which allow both the inhibitor and receptor binding pocket to ‘flex’; during docking. Finally the docking results were minimized with the Tripos force field, defining monomers outside 5 angstrom area around the inhibitor as an aggregate. The results of **11**, one of the most potent compounds of this study, are shown in Figure 1.

The nitromethylsulfonyl moiety was positioned for potential reversible participation (H-bonds) with nucleophilic residues on the aldose reductase in the charge transfer pocket of the inhibitor binding site (distance from NO<sub>2</sub> to Tyr 48-OH = 3.204 Å, angle = 163°; distance from SO<sub>2</sub> to Trp 111-NH = 2.758 Å, angle = 161°, distance from SO<sub>2</sub> to His 110-ε NH = 2.941 Å, angle = 125°). It could be considered that the nitromethylsulfonyl group, like hydantoin or carboxyl groups, is a functional moiety which is susceptible to reversible nucleophilic attack by aldose reductase.<sup>11,16</sup>

The benzene ring of the inhibitor was located between Val 47 and Trp 20, to keep hydrophobic interaction with lipophilic region of the enzyme (shortest distance from Val 47 = 3.810 Å; distance from Trp 20 = 3.908 Å). The hydrophobic interaction of *N*-methyl moiety of **11** with Phe 122, Trp 20 and Trp 219 (shortest distances are 4.813, 4.353 and 4.056 Å, respectively), no such interaction in the case of *N*-methyl unsubstituted analogue **10** (Fig. 2), led to an enhancement of inhibition activity of **11** compared with **10**. In addition, the FlexiDock

Table 1. Inhibitory activities of novel nitromethylsulfonylanilide ARIs

Compound							IC <sub>50</sub> (μM) <sup>a</sup>
	R <sub>1</sub>	R <sub>2</sub>	R <sub>3</sub>	R <sub>4</sub>	R <sub>5</sub>	R <sub>6</sub>	
<b>1</b>	H	H	H	H	H	H	6.4
<b>2</b>	Me	H	H	H	H	H	0.7
<b>3</b>	Et	H	H	H	H	H	5.9
<b>4</b>	H	H	H	Cl	H	H	4.9
<b>5</b>	Me	H	H	Cl	H	H	0.6
<b>6</b>	H	OMe	H	OMe	H	H	20.3
<b>7</b>	Me	OMe	H	OMe	H	H	2.0
<b>8</b>	H	Me	H	H	OMe	H	1.2
<b>9</b>	Me	Me	H	H	OMe	H	0.3
<b>10</b>	H	F	H	H	Me	H	2.8
<b>11</b>	Me	F	H	H	Me	H	0.35
<b>12</b>	H	Me	H	H	H	Me	2.7
<b>13</b>	H	<i>i</i> -Pr	H	H	H	<i>i</i> -Pr	> 100 <sup>b</sup>
<b>14</b>							> 100 <sup>b</sup>
SG210 <sup>c</sup>							0.1

<sup>a</sup>Inhibitory activity against recombinant human muscle cell AR.

<sup>b</sup>No significant activity at 1 × 10<sup>−4</sup> M.

<sup>c</sup>Ref 13.

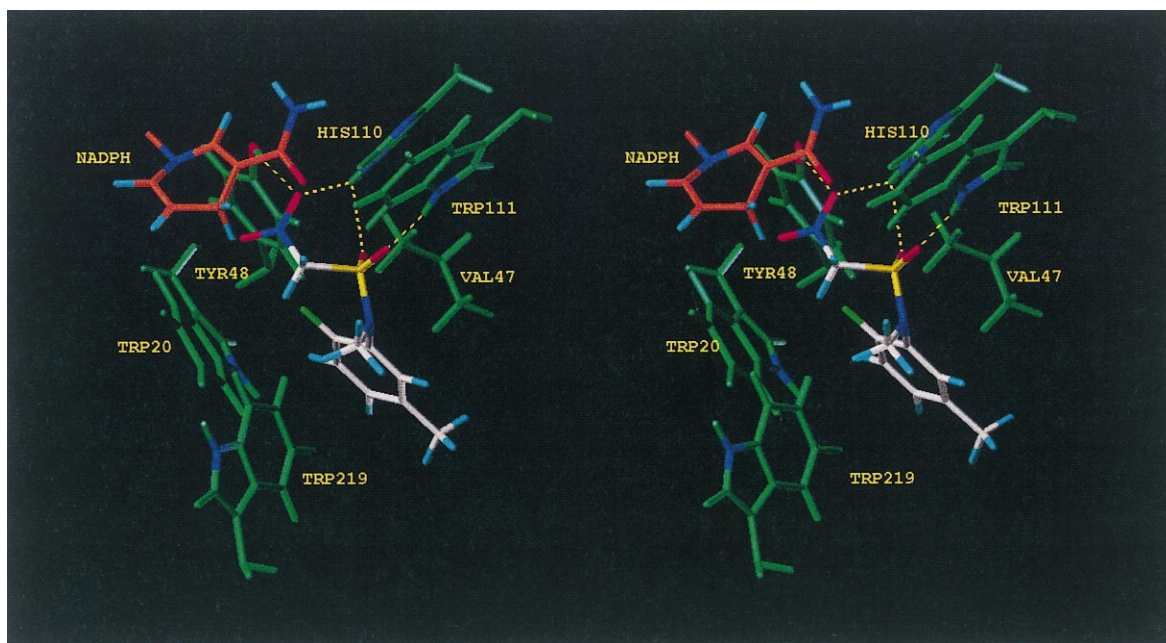


**Figure 1.** Stereoview of the most stable docking model for (2-fluoro-5-methyl-*N*-methyl)-*N*-nitromethylsulfonamide, **11** within the substrate pocket of aldose reductase. Intermolecular hydrogen bonds (distances less than 2.8 Å between the hydrogen bonded to a H-bond donor and an acceptor) are shown in dotted yellow lines. Carbon atoms are shown in white except those of the surrounding amino acids (green) and NADPH (brown). Hydrogen atoms are shown in cyan except those of the amino acids (green). Nitrogens are blue, oxygens are red, sulfur is yellow, and fluorine is light green.

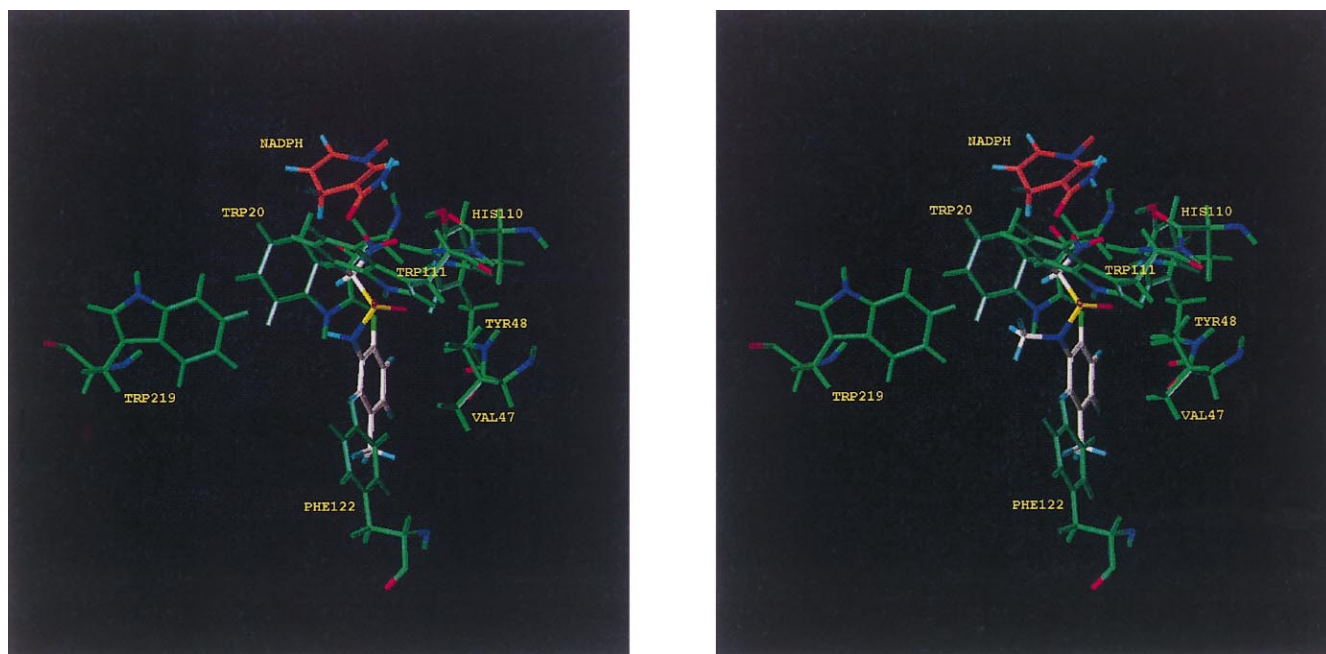


**Figure 2.** Detailed view of the most stable docking model for **11** (right) and **10** (left) within the substrate pocket of aldose reductase.

energy of **11** (−682.9 kcal/mol) was much lower than that of **10** (−470.3 kcal/mol). As a scoring function in FlexiDock, better fits simply give a lower energy of interaction. Actually, all of the compounds with a methyl moiety substituted on the nitrogen atom which bears the nitromethylsulfonyl group, exhibited better inhibition activity than the respective non-methyl substituted ones (activities: **2** > **1**; **5** > **4**; **7** > **6**; **9** > **8**; **11** > **10**). While the methyl group was replaced with an ethyl moiety, the activity decreased (activity: **2** > **3**). Similar results were

observed when bulky substituents were substituted on the benzene ring (activity: **12** > > **13**). This result might be assigned to the bulky substituents interfering with the H-bond interactions between the nitromethylsulfonyl moiety and proton donor moieties of the enzyme.

Kinetic studies of the inhibition of recombinant aldose reductase by (2-fluoro-5-methyl-*N*-methyl)-*N*-nitromethylsulfonamide, **11** was conducted with DL-glyceraldehyde as substrate.<sup>17</sup> Parallel slopes were obtained

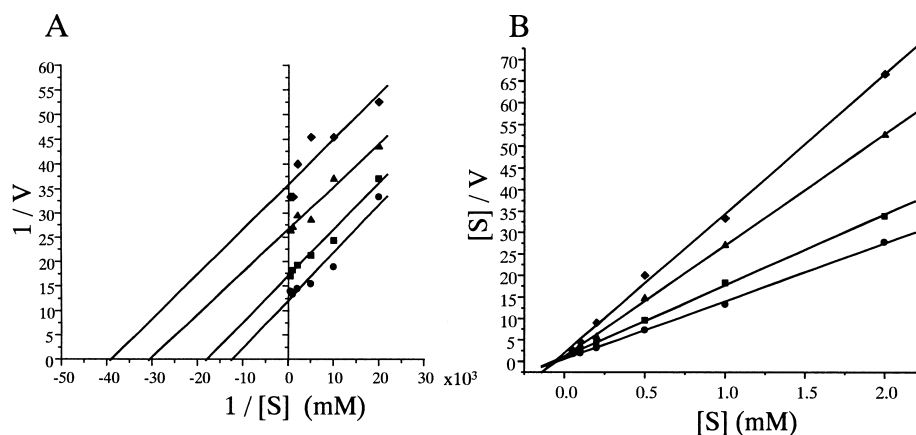


**Figure 3.** Lineweaver–Burke plot (A) and Hanes–Woolf plot (B) of the inhibition of human recombinant AR by **11** with varying concentrations of DL-glyceraldehyde as substrate. The concentrations of **11** were: ●, 0  $\mu$ M; ■, 0.02  $\mu$ M; ▲, 0.04  $\mu$ M; ◆, 0.06  $\mu$ M. S represents the substrate, DL-glyceraldehyde, while V is the measured decrease per minute in the UV absorption of NADPH at 340 nm.

on a Lineweaver–Burke plot (Fig. 3A) when the concentration of inhibitor was varied indicating that the observed inhibition of **11** was uncompetitive with glyceraldehyde as substrate. This uncompetitive inhibition was confirmed by a Hanes–Woolf plot of  $[S]/V$  versus  $[S]$  (Fig. 3B).

(2-Fluoro-5-methyl-N-methyl)-N-nitromethylsulfonamide, **11** was also evaluated for its ability to inhibit sugar cataract formation induced in intact rat lenses cultured in vitro in media containing 30% xylose.<sup>18</sup> After 48 h culture in the xylose medium, the changes in lens opacity

were photographed under a dissecting microscope. As illustrated in Figure 4, lenses remained clear when incubated in normal medium (upper-left, normal lens) while similar lenses cultured in the presence of 30% xylose formed lens opacities associated with sugar cataract formation (upper-right, cataract lens). Addition of 1 and 10  $\mu$ M of **11** to the xylose medium resulted in a dose-dependent reduction lens opacities caused by sugar cataract formation (Fig. 4, lower-left and right). Lens density

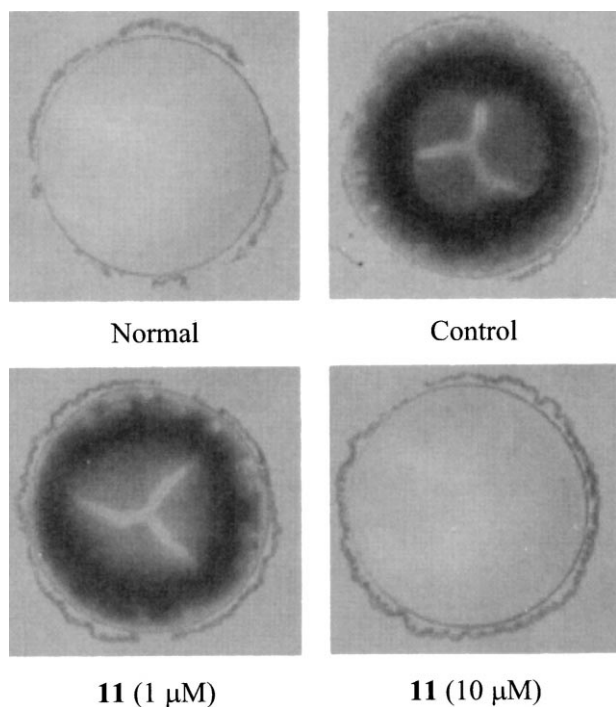


**Figure 4.** Representative appearance of lenses cultured for 2 days with and without 30% xylose and treatment with **11**. The upper-left is a normal lens cultured without xylose. The upper-right is a lens cultured in medium containing 30% xylose while the lower left and right lenses are lenses cultured in medium containing 30% xylose and 1 and 10  $\mu$ M of **11**, respectively. Darker areas indicate increased opacity due to sugar cataract accumulation.

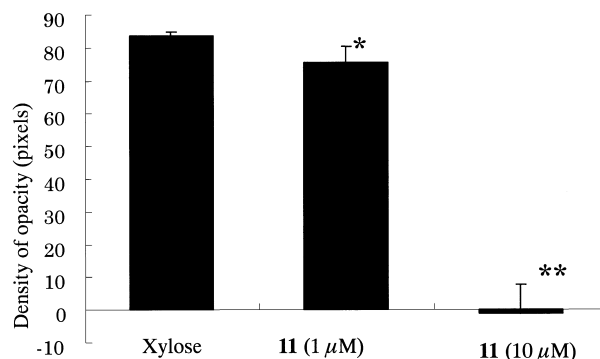


**Figure 5.** Measured opacities (optical densities) in lenses resulting from xylose induced sugar cataract formation and its reduction by treatment with **11**. Data are means  $\pm$  S.D. ( $n=5$ ). \* $P < 0.05$ , \*\* $P < 0.01$  relative to xylose.

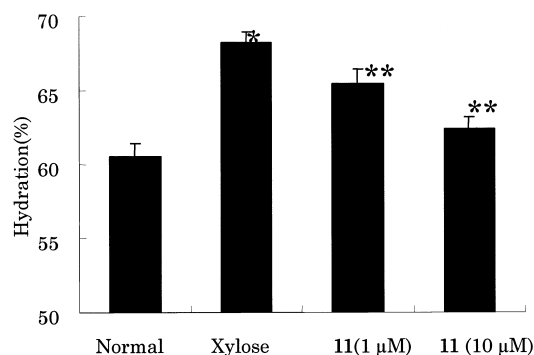


**Figure 6.** Increased hydration in xylose-induced sugar cataractous lens after 2 days of culture and the reduction of hydration in similar lenses treated with **11**. Data are means  $\pm$  S.D. ( $n=5$ ). \* $P < 0.01$  relative to normal lens, and \*\* $P < 0.01$  relative to untreated xylose lens.

measurements using computer imaging analysis confirmed that **11** was effective in reducing the total lens opacity ( $P < 0.01$ , Fig. 5). In addition, measurement of lens water levels indicated that  $10\text{ }\mu\text{M}$  **11** significantly reduced polyol associated lens hydration ( $P < 0.01$ , Fig. 6).

### Conclusions

This new series of *N*-nitromethylsulfonanilide derivatives inhibited recombinant human muscle aldose reductase in vitro with  $\text{IC}_{50}$  values ranging from 20.3 to  $0.3\text{ }\mu\text{M}$ .

Computational docking simulation analysis showed that the nitromethylsulfonyl group was positioned for potential reversible participation with nucleophilic residues on the aldose reductase in the charge transfer pocket of the inhibitor binding site. Increased hydrophobic interaction of the *N*-methyl moiety led to enhanced inhibition and the benzene ring of the inhibitor appears to be important for hydrophobic interaction with a lipophilic region on the aldose reductase.

Kinetic analysis of (2-fluoro-5-methyl-*N*-methyl)-*N*-nitromethylsulfonanilide, **11**, one of the most potent compounds with an  $\text{IC}_{50} = 0.35\text{ }\mu\text{M}$ , showed uncompetitive inhibition. Compound **11** also effectively prevented lens opacity formation and reduced lens hydration caused by sugar cataract formation in rat lens cultured in vitro in medium containing 30% xylose. These results indicate that this series of aldose reductase inhibitors are effective in delaying or preventing cataract formation in diabetes.

### Experimental

#### Chemistry

Melting points (mp) were obtained using a Yanaco Micro Melting Point Apparatus and were uncorrected. Elemental analyses were measured with a Perkin Elmer CHNS/02400 analyzer and mass spectra analyses were performed by Takeda Analytical Research Laboratories, Ltd. All indicated analyses were within  $\pm 0.4\%$  of theoretical values. NMR spectra were measured using a Varian Gemini-300 spectrometer (300 MHz for  $^1\text{H}$ , 75 MHz for  $^{13}\text{C}$ , and 282 MHz for  $^{19}\text{F}$ , respectively), and the chemical shifts are expressed in  $\delta$  (ppm) units with tetramethylsilane as an internal standard for  $^1\text{H}$  and  $^{13}\text{C}$  NMR, and with trifluoromethylbenzene as internal standard for  $^{19}\text{F}$  NMR. Unless stated otherwise, column chromatography was conducted on silica gel Merk-60 with a mixture of EtOAc and hexane as eluent.

Starting anilines or *N*-alkylanilines were commercially available or prepared according to a published method.<sup>19</sup>

#### General preparation of *N*-nitromethylsulfonanilide

Methanesulfonyl chloride (1.1 equiv) was added dropwise to a stirred solution containing 1.0 equiv aniline (or *N*-alkylaniline) and triethylamine (1.5 equiv) in  $\text{CH}_2\text{Cl}_2$  (or DMF) under ice–water cooling and the mixture was

stirred overnight at rt. Water was added to the reaction solution, and the mixture was extracted with  $\text{CH}_2\text{Cl}_2$ . The organic layer was washed with 1N HCl and then brine, and dried over anhydrous  $\text{Na}_2\text{SO}_4$ . After filtration, the solvent was evaporated in vacuo.

To a dry THF solution containing 1 equiv of the above obtained *N*-methylsulfonanilide (or *N*-methyl-*N*-methylsulfonanilide) at  $-10^\circ\text{C}$  under a nitrogen atmosphere was dropwise added 2.4 equiv (or 1.2 equiv in the case of *N*-methyl-*N*-methylsulfonanilide) of *n*-butyllithium (1.6 mol/L in hexane). The mixture was stirred for 10 min, and then cooled to  $-30^\circ\text{C}$  and isoamyl nitrate (2.2 equiv, or 1.1 equiv in the case of *N*-methyl-*N*-methylsulfonanilide) was then dropwise added. After stirring for 4 h at the same temperature, the reaction was quenched with water, and the volatiles were evaporated in vacuo. 1N NaOH (2 equiv) was added to the reaction mixture and the mixture was washed with ethyl ether. The aqueous layer was acidified with acetic acid ( $\text{pH} = 5$ ), and extracted with  $\text{CH}_2\text{Cl}_2$ . The organic layer was washed with brine and dried over anhydrous  $\text{Na}_2\text{SO}_4$ . Following filtration, the solvent was evaporated in vacuo, and the residue was purified by column chromatography and recrystallization to give the desired compounds.

***N*-Nitromethylsulfonanilide (1).** Overall yield, 7%. Colorless crystals, mp  $91.8\text{--}92.4^\circ\text{C}$  (48% EtOH).  $^1\text{H}$  NMR ( $\text{CDCl}_3$ ):  $\delta$  5.43 (2H, s), 7.12 (1H, br s), 7.30–7.46 (5H, m).  $^{13}\text{C}$  NMR ( $\text{CDCl}_3$ ):  $\delta$  82.9, 123.2 (2C), 127.2 (2C), 129.7, 129.9. Anal. calcd for  $\text{C}_7\text{H}_8\text{N}_2\text{O}_4\text{S}$ : C, 38.89; H, 3.73; N, 12.96. Found: C, 39.11; H, 3.69; N, 12.81.

***N*-Methyl-*N*-nitromethylsulfonanilide (2).** Overall yield, 17%. Colorless crystals, mp  $50.0\text{--}51.0^\circ\text{C}$  (95% EtOH).  $^1\text{H}$  NMR ( $\text{CDCl}_3$ ):  $\delta$  3.47 (3H, s), 5.45 (2H, s), 7.37–7.54 (5H, m).  $^{13}\text{C}$  NMR ( $\text{CDCl}_3$ ):  $\delta$  41.0, 83.7, 127.6 (2C), 128.9, 129.9 (2C), 139.3. Anal. calcd for  $\text{C}_8\text{H}_{10}\text{N}_2\text{O}_4\text{S}$ : C, 41.73; H, 4.38; N, 12.17. Found: C, 41.79; H, 4.36; N, 12.22.

***N*-Ethyl-*N*-nitromethylsulfonanilide (3).** Overall yield, 13%. A yellow oil.  $^1\text{H}$  NMR ( $\text{CDCl}_3$ ):  $\delta$  1.14 (3H, t,  $J = 7.2\text{ Hz}$ ), 3.84 (2H, q,  $J = 7.2\text{ Hz}$ ), 5.44 (2H, s), 7.39–7.49 (5H, m).  $^{13}\text{C}$  NMR ( $\text{CDCl}_3$ ):  $\delta$  14.9, 49.3, 84.2, 129.4, 129.6 (2C), 130.1 (2C), 137.0. Anal. calcd for  $\text{C}_9\text{H}_{12}\text{N}_2\text{O}_4\text{S}$ : C, 44.26; H, 4.95; N, 11.47. Found: C, 44.30; H, 4.95; N, 11.52.

**(4-Chloro)-*N*-nitromethylsulfonanilide (4).** Overall yield, 4%. Colorless crystals, mp  $117.7\text{--}118.3^\circ\text{C}$  (79% EtOH).  $^1\text{H}$  NMR ( $\text{CDCl}_3$ ):  $\delta$  5.43 (2H, s), 7.11 (1H, br s), 7.31–7.34 (2H, m), 7.38–7.43 (2H, m).  $^{13}\text{C}$  NMR ( $\text{CDCl}_3$ ):  $\delta$  82.5, 125.0 (2C), 130.2 (2C), 132.7, 133.7. Anal. calcd for  $\text{C}_7\text{H}_7\text{ClN}_2\text{O}_4\text{S}$ : C, 33.54; H, 2.81; N, 11.18. Found: C, 33.68; H, 2.77; N, 11.13.

**(4-Chloro-*N*-methyl)-*N*-nitromethylsulfonanilide (5).** Overall yield, 17%. Colorless crystals, mp  $106.0\text{--}106.5^\circ\text{C}$  (EtOH/ $\text{CH}_2\text{Cl}_2$ , 3:1, v/v).  $^1\text{H}$  NMR ( $\text{CDCl}_3$ ):  $\delta$  3.44 (3H, s), 5.44 (2H, s), 7.41–7.48 (4H, m).  $^{13}\text{C}$  NMR ( $\text{CDCl}_3$ ):  $\delta$  40.9, 83.7, 128.9 (2C), 130.1 (2C), 134.9, 137.8. Anal. calcd for  $\text{C}_8\text{H}_9\text{ClN}_2\text{O}_4\text{S}$ : C, 36.30; H, 3.43; N, 10.58. Found: C, 36.37; H, 3.36; N, 10.54.

**(2,4-Dimethoxy)-*N*-nitromethylsulfonanilide (6).** Overall yield, 8%. Colorless crystals, mp 91.0–91.8 °C (95% EtOH).  $^1\text{H}$  NMR ( $\text{CDCl}_3$ ):  $\delta$  3.81 (3H, s), 3.85 (3H, s), 5.44 (2H, s), 6.47–6.50 (2H, m), 7.02 (1H, br s), 7.39 (1H, m).  $^{13}\text{C}$  NMR ( $\text{CDCl}_3$ ):  $\delta$  55.6, 55.9, 83.5, 99.2, 104.9, 116.2, 126.4, 152.9, 160.0. Anal. calcd for  $\text{C}_9\text{H}_{12}\text{N}_2\text{O}_6\text{S}$ : C, 39.13; H, 4.38; N, 10.14. Found: C, 39.45; H, 4.39; N, 10.09.

**(2,4-Dimethoxy-*N*-methyl)-*N*-nitromethylsulfonanilide (7).** Overall yield, 8%. Colorless crystals, mp 115.0–116.0 °C (EtOH/ $\text{CH}_2\text{Cl}_2$ , 1:1, v/v).  $^1\text{H}$  NMR ( $\text{CDCl}_3$ ):  $\delta$  3.33 (3H, s), 3.82 (3H, s), 3.86 (3H, s), 5.54 (2H, s), 6.48–6.51 (2H, m), 7.28 (1H, m).  $^{13}\text{C}$  NMR ( $\text{CDCl}_3$ ):  $\delta$  39.7, 55.6, 55.7, 85.5, 99.6, 105.2, 120.2, 132.4, 156.6, 161.6. Anal. calcd for  $\text{C}_{10}\text{H}_{14}\text{ClN}_2\text{O}_6\text{S}$ : C, 41.37; H, 4.86; N, 9.65. Found: C, 41.72; H, 4.98; N, 9.88.

**(5-Methoxy-2-methyl)-*N*-nitromethylsulfonanilide (8).** Overall yield, 6%. Colorless crystals, mp 90.0–91.0 °C (95% EtOH).  $^1\text{H}$  NMR ( $\text{CDCl}_3$ ):  $\delta$  2.33 (3H, s), 3.80 (3H, s), 5.54 (2H, s), 6.78 (1H, m), 6.83 (1H, br s), 7.09 (1H, m), 7.19 (1H, m). Anal. calcd for  $\text{C}_9\text{H}_{12}\text{N}_2\text{O}_5\text{S}$ : C, 41.53; H, 4.65; N, 10.76. Found: C, 41.87; H, 4.74; N, 10.41.

**(5-Methoxy-2-methyl-*N*-methyl)-*N*-nitromethylsulfonanilide (9).** Overall yield, 4%. Colorless oil.  $^1\text{H}$  NMR ( $\text{CDCl}_3$ ):  $\delta$  2.33 (3H, s), 3.34 (3H, s), 3.81 (3H, s), 5.57 (2H, br s), 6.89 (1H, m), 7.05 (1H, m), 7.24 (1H, m).  $^{13}\text{C}$  NMR ( $\text{CDCl}_3$ ):  $\delta$  17.2, 40.9, 55.5, 84.7, 113.3, 114.9, 130.3, 132.6, 138.7, 158.8. HRMS:  $\text{C}_{10}\text{H}_{14}\text{N}_2\text{O}_5\text{S}$  ( $\text{M}^+$ ), calcd 274.0623; found 274.0604.

**(2-Fluoro-5-methyl)-*N*-nitromethylsulfonanilide (10).** Overall yield, 5%. Colorless crystals, mp 93.3–93.8 °C (86% EtOH).  $^1\text{H}$  NMR ( $\text{CDCl}_3$ ):  $\delta$  2.35 (3H, s), 5.54 (2H, s), 7.05–7.08 (2H, m), 7.10 (1H, m), 7.35 (1H, m).  $^{13}\text{C}$  NMR ( $\text{CDCl}_3$ ):  $\delta$  20.9, 83.7, 115.9 (1C, d,  $J=77.7$  Hz), 122.0 (1C, d,  $J=48.6$  Hz), 124.8, 128.8 (1C, d,  $J=29.1$  Hz), 135.3 (1C, d,  $J=15.6$  Hz), 152.9 (1C, d,  $J=97.6$  Hz).  $^{19}\text{F}$ -NMR ( $\text{CDCl}_3$ ):  $\delta$  –132.8. Anal. calcd for  $\text{C}_8\text{H}_9\text{FN}_2\text{O}_4\text{S}$ : C, 38.71; H, 3.65; N, 11.29. Found: C, 38.95; H, 3.62; N, 11.22.

**(2-Fluoro-5-methyl-*N*-methyl)-*N*-nitromethylsulfonanilide (11).** Overall yield, 4%. Colorless crystals, mp 76.0–77.0 °C (95% EtOH).  $^1\text{H}$  NMR ( $\text{CDCl}_3$ ):  $\delta$  2.35 (3H, s), 3.41 (3H, s), 5.56 (2H, s), 7.08 (1H, m), 7.19 (1H, m), 7.26 (1H, m).  $^{13}\text{C}$  NMR ( $\text{CDCl}_3$ ):  $\delta$  20.6, 40.3, 85.4, 116.6 (1C, d,  $J=20.0$  Hz), 126.2 (1C, d,  $J=12.2$  Hz), 131.7 (1C, d,  $J=7.8$  Hz), 131.7, 135.4, 157.0 (1C, d,  $J=248.2$  Hz).  $^{19}\text{F}$  NMR ( $\text{CDCl}_3$ ):  $\delta$  –126.5. Anal. calcd for  $\text{C}_9\text{H}_{11}\text{FN}_2\text{O}_4\text{S}$ : C, 41.22; H, 4.23; N, 10.68. Found: C, 41.24; H, 4.24; N, 10.57.

**(2,6-Dimethyl)-*N*-nitromethylsulfonanilide (12).** Overall yield, 5%. Colorless crystals, mp 125.8–126.6 °C (95% EtOH).  $^1\text{H}$  NMR ( $\text{CDCl}_3$ ):  $\delta$  2.42 (6H, s), 5.61 (2H, s), 6.50 (1H, br s), 7.12–7.22 (3H, m).  $^{13}\text{C}$  NMR ( $\text{CDCl}_3$ ):  $\delta$  19.2, 87.0, 129.0 (2C), 129.1 (2C), 131.2, 137.8. Anal. calcd for  $\text{C}_9\text{H}_{12}\text{N}_2\text{O}_4\text{S}$ : C, 44.26; H, 4.95; N, 11.47. Found: C, 44.61; H, 4.99; N, 11.39.

**(2,6-Diisopropyl)-*N*-nitromethylsulfonanilide (13).** Overall yield, 11%. Colorless crystals, mp 165.0–166.0 °C

(95% EtOH).  $^1\text{H}$  NMR ( $\text{CDCl}_3$ ):  $\delta$  1.26 (12H, d,  $J=6.9$  Hz), 3.40 (2H, m), 5.63 (2H, s), 6.48 (1H, br s), 7.21–7.26 (2H, m), 7.38 (1H, m).  $^{13}\text{C}$  NMR ( $\text{CDCl}_3$ ):  $\delta$  24.0 (4C), 28.9 (2C), 86.6, 124.5 (2C), 127.9, 130.0, 148.5 (2C). Anal. calcd for  $\text{C}_{13}\text{H}_{20}\text{N}_2\text{O}_4\text{S}$ : C, 51.98; H, 6.71; N, 9.33. Found: C, 52.19; H, 6.75; N, 9.45.

**4,5-Dimethyl-2-(nitromethylsulfonfylamino)thiazole (14).** Overall yield, 3%. Colorless crystals, mp 183.0–184.0 °C (EtOH).  $^1\text{H}$  NMR ( $\text{DMSO}-d_6$ ):  $\delta$  2.05 (3H, s), 2.11 (3H, s), 5.96 (2H, s), 12.89 (1H, br s).  $^{13}\text{C}$  NMR ( $\text{DMSO}-d_6$ ):  $\delta$  10.6, 10.8, 88.0, 114.0, 128.8, 167.9. Anal. calcd for  $\text{C}_6\text{H}_9\text{N}_3\text{O}_4\text{S}_2$ : C, 28.68; H, 3.80; N, 16.16. Found: C, 28.29; H, 3.59; N, 16.55.

## Modeling and docking simulation

Docking simulation were performed with the SYBYL 6.6 software package<sup>20</sup> running on a Silicon Graphics Iris workstation.

## Biology

**Enzyme assay.** Aldose reductase activity was determined spectrophotometrically by monitoring the oxidation of NADPH in a reaction mixture containing 100 mM sodium phosphate buffer, pH 6.2, 10 mM DL-glyceraldehyde, 0.3 mM  $\beta$ -NADPH, 0.01 unit/mL recombinant human muscle aldose reductase, and various concentrations of inhibitor. (The enzyme was purified from the culture medium of the baculovirus-insect cell line 32d gene expression system in which the c-DNA containing the entire protein coding region of human aldose reductase is expressed and the enzyme retains the same properties exhibited by human muscle and retina.) Non-inhibitor samples were run as controls and non-enzyme samples were run as Blanks.

The reduction was initiated by the addition of NADPH solution and incubated for 5 min. The absorbency of the plate was read on a microplate reader (LabSystems Multiscan Multisoft) at 340 nm.<sup>11</sup> Appropriate controls were employed to negate potential changes in the absorption of nucleotide and/or protein modification reagents or aldose reductase inhibitors at 340 nm in the absence of substrate. Under these conditions the NADPH oxidation was linear with time. Each inhibitor concentration was tested in duplicate, and an  $\text{IC}_{50}$  value for each compound was obtained from linear regression analyses of the log concentration versus percent inhibition plots of the data.<sup>21</sup>

**Kinetic studies.** A mixture of **11** (2  $\mu\text{L}$ ), 0.25 M sodium phosphate buffer (98  $\mu\text{L}$ ), varying concentrations of DL-glyceraldehyde (50  $\mu\text{L}$ ), recombinant aldose reductase (0.05 unit/mL, 50  $\mu\text{L}$ ), and 1.5 mM NADPH (50  $\mu\text{L}$ ) was incubated for 5 min. The velocity ( $V$ ) of decrease in the UV absorption of NADPH at 340 nm was recorded on the microplate reader as described above. Lineweaver–Burke plots of  $1/S$  (concentration of DL-glyceraldehyde substrate, mM) versus  $1/V$  (UV absorbency of NADPH per minute) were obtained at measuring different concentrations of **11** and DL-glyceraldehyde.



**In vitro inhibition of lens opacity.** Sugar cataract formation was induced in lenses from 4-week-old Sprague–Dawley rats by culturing at 37°C under 5% CO<sub>2</sub> atmosphere in medium containing 30% xylose. Lenses were carefully dissected from enucleated eyes by a posterior approach and checked for potential dissection damage by pre-incubation in 4 mL of Eagles essential medium containing 10% fetal calf serum. After 24 h remaining clear lenses were carefully transferred to similar medium containing 30% xylose with and without the aldose reductase inhibitor **11**. After 48 h culture in the xylose containing medium, each lens was photographed under a dissecting microscope and the clarity of each lens was quantified using computerized imaging analysis (Image 1.31 software, Twilight clone BBC, Silver Springs, MD).

**Measurement of water content and hydration rate.** Each lens was weighed immediately after incubation (wet weight, W<sub>w</sub>) and after drying at 100°C for 16 h (W<sub>d</sub>). The percent lens hydration was calculated using the equation:

$$\% \text{ Hydration} = [(W_w - W_d)/W_w] \times 100\%.$$

#### Acknowledgement

The authors thank Dr. Yutaka Kawamatsu (Senju) for his helpful advice.

#### References

1. Kador, P. F. *Med. Res. Rev.* **1988**, 8, 325–352.
2. Dvornic, D. In *Aldose Reductase Inhibition: An Approach to the Prevention of Diabetic Complications*, McGraw Hill: New York, 1987, 368.
3. Tomlinson D. R.; Stevens E. J.; Diemel L. T. *Trends Pharmacol. Sci.* **1994**, 293.
4. Kador, P. F.; Kinoshita, J. H.; Sharpless, N. E. *J. Med. Chem.* **1985**, 28, 841.
5. Kador, P. F.; Robinson, W. G.; Kinoshita, J. H. *Annu. Rev. Pharmacol. Toxicol.* **1985**, 25, 691.
6. Sima, A. A. F.; Bril, V.; Nathaniel, T. A.; McEwen, J.; Brown, M. B.; Lattimet, S. A.; Green, D. A. *N. Engl. J. Med.* **1988**, 319, 548.
7. Mylary, B. L.; Larson, E. R.; Beyer, T. A.; Zembrowski, W. J.; Aldinger, C. E.; Dee, M. F.; Siegel, T. W.; Singleton, D. H. *J. Med. Chem.* **1991**, 34, 108.
8. Humber L. G. In *Progress in Medicinal Chemistry: The Medicinal Chemistry of Aldose Reductase Inhibitors*; Ellis G.P.; West, G. B. Eds.; Elsevier Science: New York, 1987; Vol. 24, pp 299–343.
9. Sarges, R. In *Advances in Drug Research: Aldose Reductase Inhibitors; Structure–Activity Relationships and Therapeutic Potential*; Academic: San Diego, 1989; Vol. 18, pp 139–175.
10. Brittain, D. R.; Brown, S. P.; Cooper, A. L.; Longridge, J. L.; Morris, J. J.; Preston, J.; Slater, L. European Patent Application **1991**, publication number: 0 469 887 A1.
11. Kador, P. F.; Sharpless, N. E. *Mol. Pharmacol.* **1983**, 24, 521.
12. Lee, Y. S.; Pearlstein, R.; Kador, P. F. *J. Med. Chem.* **1994**, 37, 787.
13. Aotsuka, T.; Hosono, H.; Kurihara, T.; Nakamura, Y.; Matsui, T.; Kobayashi, F. *Chem. Pharm. Bull.* **1994**, 42, 1264.
14. Harrison, D. H.; Bohren, K. M.; Ringe, D.; Petsgo, G. A.; Gabbay, K. H. *Biochemistry* **1994**, 33, 2011.
15. Powell, M. J. D. *Math. Program.* **1977**, 12, 241.
16. Rarey, M.; Kramer, B.; Lengauer, T.; Klebe, G. *J. Mol. Biol.* **1996**, 261, 470.
17. Kinoshita, J. H.; Kador, P. F.; Datiles, M. D. *J. Am. Med. Assoc.* **1981**, 246, 257.
18. Azuma, M.; Inoue, E.; Oka, T. *Curr. Eye Res.* **1995**, 14, 27.
19. Roberts, R. M.; Vogt, P. J. *Org. Syntheses* **1963**, 3, 420.
20. SYBYL 6.6; 1999; Tripos Associates, 1699 S. Hanley Road, Suite 303, St. Louis, MO 63144.
21. Sato, S.; Old, S.; Carper, D.; Kador, P. F. *Adv. Exp. Med. Biol.* **1995**, 372, 259.